physical sciences forum

Proceeding Paper

A Bayesian Data Analysis Method for an Experiment to Measure the Gravitational Acceleration of Antihydrogen

Danielle Hodgkinson, Joel Fajans and Jonathan S. Wurtele

MDPI

https://doi.org/10.3390/psf2023009009

physical sciences forum

MDPI

Proceeding Paper

A Bayesian Data Analysis Method for an Experiment to Measure the Gravitational Acceleration of Antihydrogen †

Danielle Hodgkinson *, Joel Fajans and Jonathan S. Wurtele

Department of Physics, University of California at Berkeley, Berkeley, CA 94720, USA; joel@physics.berkeley.edu (J.F.); wurtele@berkeley.edu (J.S.W.)

* Correspondence: danielle.louise.hodgkinson@cern.ch

† Presented at the 42nd International Workshop on Bayesian Inference and Maximum Entropy Methods in Science and Engineering, Garching, Germany, 3–7 July 2023.

Abstract: The ALPHA-g experiment at CERN intends to observe the effect of gravity on antihydrogen. In ALPHA-g, antihydrogen is confined to a magnetic trap with an axis aligned parallel to the Earth's gravitational field. An imposed difference in the magnetic field of the confining coils above and below the trapping region, known as a bias, can be delicately adjusted to compensate for the gravitational potential experienced by the trapped anti-atoms. With the bias maintained, the magnetic fields of the coils can be ramped down slowly compared to the anti-atom motion; this releases the antihydrogen and leads to annihilations on the walls of the apparatus, which are detected by a position-sensitive detector. If the bias cancels out the gravitational potential, antihydrogen will escape the trap upwards or downwards with equal probability. Determining the downward (or upward) escape probability, p, from observed annihilations is non-trivial because the annihilation detection efficiency may be up–down asymmetric; some small fraction of antihydrogen escaping downwards may be detected in the upper region (and vice versa) meaning that the precise number of trapped antihydrogen atoms is unknown. In addition, cosmic rays passing through the apparatus lead to a background annihilation rate, which may also be up–down asymmetric. We present a Bayesian method to determine p by assuming annihilations detected in the upper and lower regions are independently Poisson distributed, with the Poisson mean expressed in terms of experimental quantities. We solve for the posterior p using the Markov chain Monte Carlo integration package, Stan. Further, we present a method to determine the gravitational acceleration of antihydrogen, a_g, by modifying the analysis described above to include simulation results. In the modified analysis, p is replaced by the simulated probability of downward escape, which is a function of a_g.

Keywords: Markov chain Monte Carlo; Stan; antimatter; CERN

Citation: Hodgkinson, D.; Fajans, J.; Wurtele, J.S. A Bayesian Data Analysis Method for an Experiment to Measure the Gravitational Acceleration of Antihydrogen. *Phys. Sci. Forum* **2023**, *9*, 9. https://doi.org/10.3390/psf2023009009

Academic Editors: Udo von Toussaint and Roland Preuss

Published: 28 November 2023

1. Introduction

The universe appears to consist almost entirely of matter with a paucity of antimatter. Known as the baryon asymmetry problem, this disparity remains one of the large outstanding questions in physics. Experiments that investigate the standard model's predictions of the fundamental properties of antimatter have the potential to illuminate this open question. The ALPHA experiment at CERN traps and probes the simplest antimatter atom—antihydrogen—to enable comparisons to the well-known properties of hydrogen. ALPHA's new apparatus, known as ALPHA-g, intends to measure the effect of gravity on trapped antihydrogen [1–3]. According to Einstein's weak equivalence principle, antihydrogen accelerates at the same rate as hydrogen in the gravitational field of the Earth; a difference in the acceleration rates would be an extraordinary observation and could lead to a new way of understanding the excess of matter in our universe.

In ALPHA, antihydrogen is created by merging antiproton and positron plasmas. A schematic of the ALPHA experiment is shown in Figure 1. Antiprotons, from CERN's antiproton decelerator, enter the experiment from the left and arrive at the antiproton catching

trap. Positrons are generated from radioactive beta decay in a Surko-type accumulator [4]. These charged plasmas are first confined by Penning–Malmberg traps; the electric field of hollow cylindrical electrodes provides axial confinement and an axial magnetic field provides radial confinement. The plasmas then travel along beamlines that are guided around the corner into the ALPHA-g atom trap by magnetic fields where they are caught in another set of Penning–Malmberg traps.

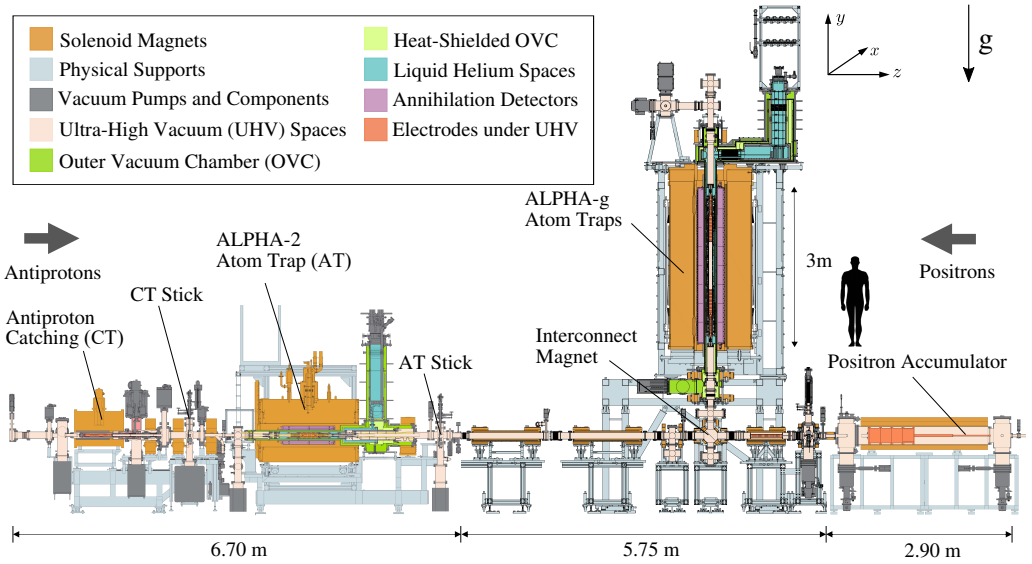

Figure 1. The ALPHA apparatus. Figure adapted from [5].

Charge-neutral antihydrogen [6] cannot be trapped with electric fields. A magnetic field configuration with a minimum magnitude at the trap center can trap antihydrogen via the interaction of its magnetic moment with the magnetic field, $\mathbf{B}$, which results in a trapping potential, $U_T = -\mu_B(|\mathbf{B}| - |\mathbf{B}_{\min}|)$, where μ_B is the Bohr magneton and $\mathbf{B}_{\min}$ is the minimum magnetic field in the trap. This configuration prevents antihydrogen from annihilating on the trap wall. The magnetic field magnitude, $|\mathbf{B}|$, which increases as a function of the radius within the trapping region, is generated by an octupole magnet and axially spaced coils. The coils confine antihydrogen axially. This magnetic 'bowl' potential is superimposed onto the Penning–Malmberg trapping fields prior to merging antiproton and positron plasmas. The merging technique forms antihydrogen in a thermal distribution with a temperature of ∼30 K. The depth of the magnetic bowl is only approximately 0.5 K; hence, most antihydrogen escapes quickly from the trap and only the fraction with the lowest energy remains confined.

The ALPHA-g superconducting magnets are shown in Figure 2. ALPHA designed the 'up–down measurement' section to measure the sign of the gravitational force on antihydrogen in the Earth's gravitational field. Initially, both the long octupole and lower short octupole are energized to provide radial antihydrogen confinement and the coils above and below the trapping regions. The 'lower' and 'upper' coils, are energized to provide axial confinement.

The experiment relies on the principle that trapped antihydrogen experiences a gravitational potential as well as a magnetic confining potential in ALPHA-g. Since the force of gravity is (in theory) parallel to the trap axis, the total potential for a trapped antihydrogen atom is

$$U(x,y,z) = -\mu_B\Big[|\mathbf{B}(x,y,z)| - |\mathbf{B}_{\min}(x,y,z)|\Big] + ma_g z, \quad (1)$$

where m is the antihydrogen mass and a_g is the parameter of interest: the antihydrogen gravitational acceleration. When the magnetic fields provided by the lower and upper coils are equal, the gravitational potential results in an up–down asymmetry in the total potential, which is shown as 'no compensation' in Figure 3. Note that Figure 3 assumes

antihydrogen behaves identically to hydrogen in the gravitational field of the Earth ($a_g = g$, where g is the hydrogen gravitational acceleration).

The magnetic fields created by the lower and upper coils can be deliberately unbalanced by supplying slightly different currents. This difference in the magnetic field magnitude, a bias, is defined as

$$\phi = \frac{\mu_B \left[|\boldsymbol{B}(x=0, y=0, z_u)| - |\boldsymbol{B}(x=0, y=0, z_l)| \right]}{m(z_u - z_l)}, \tag{2}$$

where z_u and z_l are the axial centers of the upper and lower coils, respectively. The bias compensates for the gravitational potential over the length of the trap and can be delicately adjusted and varied over different experimental trials. Some biases will overcompensate for the gravitational potential and others will undercompensate, as shown in Figure 3. When the gravitational force is perfectly compensated, the total potential is up–down symmetric.

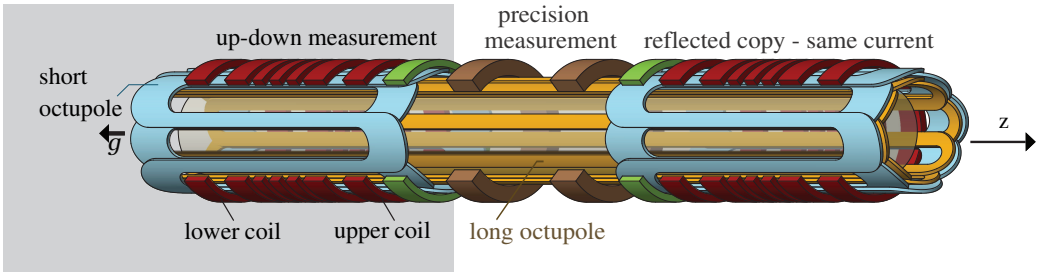

Figure 2. ALPHA-g superconducting magnets. The diagram is rotated such that the gravitational force points to the left. For the experiment described in the text, antihydrogen is confined in the 'up–down measurement' region with magnetic potential produced initially by energising the long octupole (yellow), short octupole (blue) and the lower and upper coils (red). Figure courtesy of Chukman So.

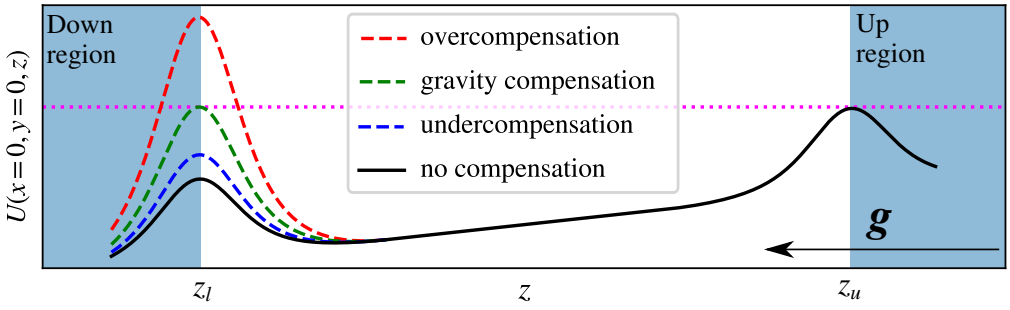

Figure 3. An exaggerated diagram of the on-axis magnetic potential during an up–down measurement. If the magnetic field produced by the lower and upper coils is equal (black solid curve), the gravitational potential leads to the (exaggerated) up/down asymmetric potential shown. By varying the relative magnetic field produced by the coils, the gravitational potential can be compensated. The red, blue and green dashed lines show varying degrees of compensation. The regions in which detected antihydrogen is considered to have escaped downwards or upwards are highlighted in blue. The centers of the lower and upper coils are marked as z_l and z_u, respectively.

To make a measurement of the gravitational potential, we must perform a controlled ramp down of the magnetic fields, during which we monitor the direction of antihydrogen escapes. As the current in both the lower and upper coils is ramped down slowly compared to the antihydrogen motion, the bias is held constant. If the total potential is not perfectly symmetric during coil ramp down, antihydrogen will preferentially escape either upwards or downwards. When antihydrogen escapes the trap, it will annihilate with the internal trap structures; these annihilations are reconstructed by a time and position-sensitive detector.

During an experimental trial, annihilations in the up and down regions (defined in Figure 3) are counted.

When performing these trials at different biases, we count the annihilations in the up and down regions to find a balance point between the bias and the gravitational potential. An equal probability to escape downwards (as opposed to upwards) indicates correct compensation of the gravitational potential. When this is achieved, you can equate a measurement of the bias with the gravitational potential.

We use standard ALPHA simulation techniques [7–9] and detailed Biot–Savart models of the ALPHA-g magnetic fields to predict the probability, p, of an individual antihydrogen atom escaping the trap downwards. At a set bias, ϕ, and a set a_g, $p \approx n_d/(n_d + n_u)$, where n_d and n_u are the simulated counts in the up and down regions, respectively. Since the full simulation results are still being analysed, Figure 4 shows estimations of p as a function of bias for $a_g = g$ ('normal gravity', green) and $a_g = -g$ ('repulsive gravity', blue), called an 'escape curve'. Note that when the imposed bias cancels the gravitational potential we have that $p = 0.5$, and the antihydrogen has equal probability of upward and downward escape. The goal of the up–down measurement is to determine the sign of the gravitational acceleration of antihydrogen by comparing an experimental escape curve to the simulation results. Determining the experimental escape curve from the data is challenging due to the following:

1. There is an experimentally limited amount of trapped antihydrogen.
2. The efficiency of detection in the up and down regions may be asymmetric.
3. Some small fraction of antihydrogen escaping downwards may be detected in the up region (and vice versa).
4. The precise number of total trapped anti-atoms is unknown experimentally.
5. Cosmic rays passing through the apparatus lead to a background annihilation rate, which may be up–down asymmetric.

In this work, we present a Bayesian data analysis method that considers the effects above and calculates the posterior p from the experimental data for a given ϕ in order to enable the experimental data to be compared to the simulation results. In addition, we present a modification of this Bayesian technique to enable a measured value to be assigned to a_g by including simulated escape curves in a likelihood analysis.

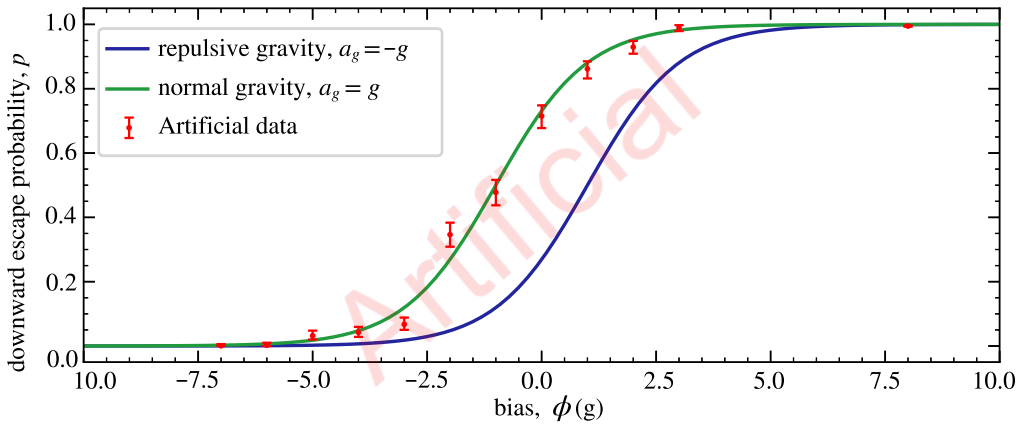

Figure 4. Estimation of simulated downward escape probability, p, as a function of bias, ϕ, for simulations assuming normal gravity ($a_g = g$, green) and repulsive gravity ($a_g = -g$, blue). Artificial data was generated using binomial sampling from the estimation of the normal gravity simulation (green line). The posterior p for the artificial data was determined using the Bayesian method described in the text. Red dots are the maximum a posteriori probability (MAP) estimate of the posterior p and the error bars are 68 % credible intervals.

2. Materials and Methods

2.1. Determining the Experimental Escape Curve

For each experimental bias, labelled with index i, our goal is to determine the posterior p_i. Our observed experimental data will be the up and down counts, $n_{u,i}$ and $n_{d,i}$, respectively. Let antihydrogen escaping the trap in the (correct) upwards (subscript u) direction be detected with efficiency η_{uu} and in the (incorrect) down (d) category with efficiency η_{du}. Similarly, antihydrogen escaping in the d direction will be detected in the correct category with efficiency η_{dd} and in the incorrect category with efficiency η_{ud}. Therefore, the detector efficiency has four components: $\boldsymbol{\eta} = (\eta_{uu}, \eta_{dd}, \eta_{du}, \eta_{ud})$.

Antihydrogen is formed in the up–down measurement trap with radial confinement provided by both the short and long octupole magnets. This maximizes the depth of the magnetic trapping potential, optimising the trapping rate. However, the superconducting windings of the long octupole (the end turns that connect the eight poles) are asymmetric about the trapping region (see Figure 2). To avoid an off-axis asymmetry in the trap magnetic fields that may mimic a bias, the long octupole is ramped down prior to the up–down measurement. This ramp down is slow compared to the anti-atom motion, meaning the antihydrogen will lose energy adiabatically [8] during the process. As a result, more antihydrogen can be trapped than by using the short octupole alone. The number of annihilations observed in the long octupole ramp down, $n_{l,i}$, provides an additional piece of information. Assuming antihydrogen is always formed in the same energy distribution in the initial trap, it provides a calibration to the total number of anti-atoms escaping during the coil ramp down. Since antihydrogen is expected to be formed in a distribution with a temperature ($\sim$30 K) that is large compared to the trap depth ($\approx$0.5 K), the energy distribution of the trapped antihydrogen is expected to be largely insensitive to fluctuations in antiproton and positron plasma conditions.

Cosmic rays passing through the apparatus can, to some extent, be distinguished from antihydrogen annihilations using reconstruction algorithms [10]. However, a small background rate of cosmic ray annihilations remains. We define this rate as having three components, $\boldsymbol{\rho} = (\rho_u, \rho_d, \rho_l)$. Components ρ_u and ρ_d are the mean cosmic ray annihilation rates in the up and down regions, respectively (see Figure 2), and ρ_l is the mean rate in the detection region for the long octupole ramp down, which spans the down region, the up region and the space in between. The mean cosmic ray annihilation rates can be measured experimentally when there are no particles trapped in the apparatus.

We assume the experimental counts ($n_{u,i}$, $n_{d,i}$ and $n_{l,i}$) are independently Poisson distributed such that the conditional probability is defined as

$$\mathrm{P}(n_{u,i}, n_{d,i,}, n_{l,i} | p_i, \boldsymbol{\rho}, \boldsymbol{\eta}, \lambda_i, \beta) = \frac{(\mu_{u,i})^{n_{u,i}}}{n_{u,i}!} e^{-\mu_{u,i}} \frac{(\mu_{d,i})^{n_{d,i}}}{n_{d,i}!} e^{-\mu_{d,i}} \frac{(\mu_{l,i})^{n_{l,i}}}{n_{l,i}!} e^{-\mu_{l,i}}, \tag{3}$$

where the Poisson means, $\mu_{u,i}$, $\mu_{d,i}$ and $\mu_{l,i}$, can be expressed in terms of p_i and the other experimental parameters,

$$\mu_{l,i} = \lambda_i + \rho_l \tau_{l,i}, \tag{4}$$

$$\mu_{u,i} = \Big[\eta_{\mathrm{uu}}\{1 - p_i\} + \eta_{\mathrm{ud}} p_i\Big] \beta \lambda_i + \rho_{\mathrm{u}} \tau_{m,i}, \tag{5}$$

$$\mu_{d,i} = \Big[\eta_{\mathrm{du}}\{1 - p_i\} + \eta_{\mathrm{dd}} p_i\Big] \beta \lambda_i + \rho_{\mathrm{d}} \tau_{m,i}, \tag{6}$$

where $\tau_{l,i}$ and $\tau_{m,i}$ represent the total duration of the long octupole and coil ramp down, respectively, and can be measured experimentally with high enough accuracy to neglect measurement uncertainty. The value λ_i is the mean number of antihydrogen atoms that are detected during the long octupole ramp down. Note that we have assumed a constant of proportionality, β, between λ_i and the mean number of antihydrogen atoms escaping during the coil ramp down that is shared between all biases.

We perform up–down measurements at $|\phi| \gg g$ to calibrate the detector efficiency. For $|\phi| \gg g$, almost all antihydrogen is expected to escape the trap downwards or upwards, depending on the sign of ϕ. Even at these extreme biases, a small fraction of anti-atoms are expected to escape in the non-preferential direction, which is likely due to a transfer of transverse to axial anti-atom energy [9] during the coil ramp down. Since the simulation predicts that some small fraction of antihydrogen will escape in the non-preferential direction, we include simulated results at these calibration biases in the likelihood analysis. The probability to observe $N_{u,j}$ and $N_{d,j}$ simulated counts in the up and down categories at a calibration bias is

$$\mathrm{P}(N_{u,j}, N_{d,j}|p_j) = \frac{(\mu_{u,j})^{N_{u,j}}}{N_{u,j}!} e^{-\mu_{u,j}} \frac{(\mu_{d,j})^{N_{d,j}}}{N_{j,c}!} e^{-\mu_{d,j}}, \tag{7}$$

with Poisson means given by

$$\mu_{u,j} = (N_{u,j} + N_{d,j})(1 - p_j) \tag{8}$$

and

$$\mu_{d,j} = (N_{u,j} + N_{d,j})p_j, \tag{9}$$

where p_j is the probability of downward escape at the calibration bias.

The likelihood for a full set of experimental data at a total of K biases, of which a subset K_c are calibration biases, is

$$\mathrm{P}(\overbrace{\{n_{u,0}, n_{d,0}, n_{l,0}\} \ldots \{n_{u,K}, n_{d,K}, n_{l,K}\}, \{N_{u,0}, N_{d,0}\} \ldots \{N_{u,K_c}, N_{d,K_c}\}}^{\mathcal{O}} | p_0 \ldots p_K, \boldsymbol{\rho}, \boldsymbol{\eta}, \lambda_0 \ldots \lambda_K, \beta) = \prod_{i=0}^{K} \mathrm{P}(n_{u,i}, n_{d,i,}, n_{l,i}|p_i, \boldsymbol{\rho}, \boldsymbol{\eta}, \lambda_i, \beta) \prod_{j=0}^{K_\mathrm{c}} \mathrm{P}(N_{u,j}, N_{d,j}|p_j), \tag{10}$$

where the expressions for the conditional probabilities on the right hand side are given by Equations (3) and (7). For simplicity, we denote the set of observed experimental data at K biases and observed simulation counts at K_c biases using the symbol $\mathcal{O}$. Bayes theorem states

$$\mathrm{P}(p_i \ldots p_K, \boldsymbol{\rho}, \boldsymbol{\eta}, \lambda_i \ldots \lambda_K, \beta|\mathcal{O}) \propto \mathrm{P}(\mathcal{O}|p_i \ldots p_K, \boldsymbol{\rho}, \boldsymbol{\eta}, \lambda_i \ldots \lambda_K, \beta)\mathrm{P}(p_i \ldots p_K, \boldsymbol{\rho}, \boldsymbol{\eta}, \lambda_i \ldots \lambda_K, \beta), \tag{11}$$

and the posterior distribution of p_i can be found by marginalising the nuisance parameters,

$$\mathrm{P}(p_i|\mathcal{O}) \propto \int d\beta \iint_{j=0\ldots K} d\lambda_j \int d\boldsymbol{\eta} \int d\boldsymbol{\rho} \iint_{j=0\ldots K, j\neq i} dp_j \, \mathrm{P}(\mathcal{O}|p_0 \ldots p_K, \boldsymbol{\rho}, \boldsymbol{\eta}, \lambda_0 \ldots \lambda_K, \beta)\mathrm{P}(p_0 \ldots p_K, \boldsymbol{\rho}, \boldsymbol{\eta}, \lambda_0 \ldots \lambda_K, \beta), \tag{12}$$

where the integrals labelled with index j represent j-dimensional integration. We assume a prior for each parameter that is independent of all other parameters such that $\mathrm{P}(p_0 \ldots p_K, \boldsymbol{\rho}, \boldsymbol{\eta}, \lambda_0 \ldots \lambda_K, \beta) = \mathrm{P}(p_0)\mathrm{P}(p_1) \ldots \mathrm{P}(\beta)$. Each p_i is assigned a conservative prior that is uniform between 0 and 1. The priors on the cosmic background annihilation rates ($\boldsymbol{\rho}$) will be informed by detector counting experiments when the particle traps are empty. The detector efficiencies ($\boldsymbol{\eta}$) are, in general, assigned uniform priors between 0 and 1, but it was necessary to pin η_{uu} to a fixed value to avoid a numerical convergence issue; this did not impact the posterior p_i. Broad uniform priors are assigned to the λ_i and β parameters. To solve for $P(p_i|\mathcal{O})$ at each bias, we use the Markov chain Monte Carlo integration package, Stan [11], which uses no-U-turn sampling [12] (NUTS). Stan libraries are available in many programming languages; we use the Python library, referred to as PyStan.

In Figure 4 we show the result for an experimental escape curve, generated using artificial data. For each of the discrete bias values that make up the artificial dataset, $p(\phi)$ is determined from the normal gravity ($a_g = g$) curve. Then, 200 binomial samples are generated in the up or down categories with probability of downward escape $p(\phi)$. With current antihydrogen accumulation rates in ALPHA-g, we anticipate approximately three days of data collection per bias to trap this amount of antihydrogen. The sampling provides a set of artificial up (n_u) and down (n_d) counts at the discrete biases. We also assume $n_l = n_u + n_d$, asserting a 1:1 relationship between the long octupole and coil ramp-down counts, which is approximately the ratio predicted by simulation. We plot the maximum a posteriori probability (MAP) estimate and 68 % credible intervals of $P(p_i|\mathcal{O})$. The artificial data curve is clearly discernible from the repulsive gravity curve with reasonable assumed experimental statistics. We have neglected the uncertainty associated with the accuracy of the measurement of the bias, which will form a horizontal error bar on the real experimental data.

2.2. Determining the Antihydrogen Gravitational Acceleration

Here we present a modified version of the likelihood analysis, in which we include simulated escape curves at a range of different assumed gravitational accelerations, a_g. Simulation results indicate that changing the assumed a_g is equivalent to translating the simulated escape curve along the bias axis. For example, the normal gravity ($a_g = g$) simulated escape curve is indistinguishable from a translation of the repulsive gravity ($a_g = -g$) curve by -2 g along the bias axis. As before, we assume counts in the up and down regions and in the long octupole ramp down, which are independently Poisson distributed, and hence the likelihood of the experimental counts is given by Equation (3) with modified Poisson means defined as

$$\mu'_{l,i} = \lambda_i + \rho_l \tau_{l,i}, \tag{13}$$

$$\mu'_{u,i} = \Big[\eta_{\mathrm{uu}}\{1 - p_{\mathrm{sim}}(\phi_i + a_g)\} + \eta_{\mathrm{ud}} p_{\mathrm{sim}}(\phi_i + a_g)\Big]\beta\lambda_i + \rho_{\mathrm{u}}\tau_{m,i}, \tag{14}$$

$$\mu'_{d,i} = \Big[\eta_{\mathrm{du}}\{1 - p_{\mathrm{sim}}(\phi_i + a_g)\} + \eta_{\mathrm{dd}} p_{\mathrm{sim}}(\phi_i + a_g)\Big]\beta\lambda_i + \rho_{\mathrm{d}}\tau_{m,i}, \tag{15}$$

where the experimental downward escape probability, p_i (see Equations (4)–(6)), has been replaced by a function, p_{sim}, which represents the simulated downward escape probability and is evaluated at the bias, ϕ_i, plus an offset, a_g. Monte Carlo simulations model the antihydrogen dynamics at discrete biases and discrete assumed gravitational accelerations. For each assumed gravitational acceleration, the simulated escape curve (containing simulations at a set of discrete biases) is translated along the bias axis to line up with the no-gravity simulation. For example, an escape curve assuming normal gravity ($a_g = g$) is translated by $-g$ along the bias axis. Finite simulation statistics lead to a spread of the simulated points about a central value, which is included by assigning a Gaussian prior to p_{sim}. The value p_{sim} is determined as a continuous function of bias using spline interpolation. Since a_g represents the offset from an assumption of no gravity it is the measured antihydrogen gravitational acceleration (the parameter of interest).

The posterior a_g can be found by applying Bayes' theorem and integrating over the nuisance parameters, similar to Equation (12). We assign a uniform prior to a_g that is significantly broader than the likely range, which can be determined by inspection of Figure 4. Again, we use a Stan [11] model to perform this calculation. Figure 5 shows the posterior probability distribution for a_g using the artificial data described in Section 2.1. The result is an antihydrogen gravitational acceleration of $a_g = 1.0^{+0.2}_{-0.1}\, g$ to one decimal place, trivially confirming that the artificial data were sampled from the escape curve with $a_g = g$.

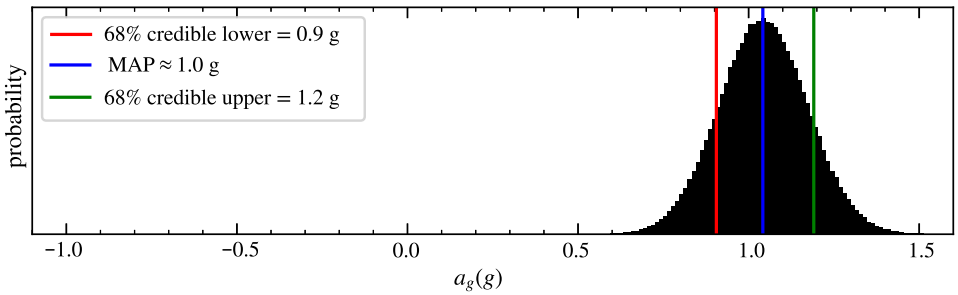

Figure 5. Posterior probability density of the gravitational acceleration of antihydrogen, a_g, for an artificial dataset. Blue and red/green vertical lines mark the maximum a posteriori probability (MAP) estimate and the 68 % credible intervals, respectively.

3. Discussion

In the ALPHA-g up–down measurement, antihydrogen will be confined by a magnetic field to enable the direction of its gravitational interaction with the Earth to be measured. An imposed difference in the magnetic field above and below the trapping region can compensate for the gravitational potential. Experimental trials involve slowly removing the magnetic confining potential with a maintained bias and counting the number of antihydrogen annihilations that are detected above and below the trapping region.

We presented a Bayesian data analysis method to determine the probability of an antihydrogen atom escaping the trap downwards, p_i, at a given bias during the experiment. Counts, detected in the regions above and below the trapping region, are assumed to be independently Poisson distributed. The method accounts for asymmetries in the efficiency by which antihydrogen annihilations are detected in the upper and lower regions of ALPHA-g, the small fraction of antihydrogen escaping downwards that may be detected in the upper region (and vice versa), the unknown number of total trapped anti-atoms and the (potentially up–down asymmetric) rates of cosmic ray annihilations. A demonstration of the method on an artificial dataset, with experimentally feasible statistics, predicts that we will be able to distinguish repulsive gravity from normal gravity. An alternative approach to this analysis [13] yields similar results.

Simulations indicate that changing the assumed value of the antihydrogen gravitational acceleration, a_g, is equivalent to translating the escape curve along the bias axis. Accordingly, we have developed a Bayesian analysis of the experimental value of a_g from the data by modifying the likelihood analysis. We applied the method to the artificial dataset, which trivially reproduces the assumed a_g. Again, the alternative approach of Ref. [13] yields similar results. The width of the posterior distribution reaffirms that $a_g = g$ and $a_g = -g$ will be distinguishable with a level of statistics that are feasibly obtainable. In this determination of a_g, we have neglected the uncertainty in the simulated magnetic fields and the unknown initial distribution of antihydrogen energies. For analysis of the real experimental data, these factors will provide an additional uncertainty in a_g that is not quantified here.

Author Contributions: Conceptualization, J.F.; methodology, D.H., J.F. and J.S.W.; software, D.H.; validation, N/A; formal analysis, D.H.; investigation, N/A; resources, J.F. and J.S.W.; data curation, N/A; writing—original draft preparation, D.H.; writing—review & editing, D.H., J.F. and J.S.W.; Visualization, D.H.; Supervision, J.F. and J.S.W.; project administration, J.F. and J.S.W.; funding acquisition, J.F. and J.S.W. All authors have read and agreed to the published version of the manuscript.

Funding: This work was supported by the DOE OFES and NSF-DOE Program in Basic Plasma Science.

Institutional Review Board Statement: Not applicable.

Informed Consent Statement: Not applicable.

Data Availability Statement: Data sharing is not applicable to this article.

Acknowledgments: We thank Andrew Charman (Department of Physics, University of California at Berkeley) for sharing his knowledge of Bayesian statistics and of the Stan programming language. We thank Karen Zukor for her edits to the language in this proceeding.

Conflicts of Interest: The authors declare no conflict of interest.

References

1. Zhmoginov, A.I.; Charman, A.E.; Shalloo, R.; Fajans, J.; Wurtele, J.S. Nonlinear dynamics of anti-hydrogen in magnetostatic traps: implications for gravitational measurements. *Class. Quantum Gravity* **2013**, *30*, 205014. [CrossRef]
2. Charman, A.E.; Amole, C.; Menary, S.; Capra, A.; Baquero-Ruiz, M.; Fajans, J.; Ashkezari, M.D.; Bertsche, W.; Butler, E.; Cesar, C.L.; et al. Description and first application of a new technique to measure the gravitational mass of antihydrogen. *Nat. Commun.* **2013**, *4*, 1785. [CrossRef]
3. Hangst, J.S. *Addendum to the ALPHA Proposal; The ALPHA-g Apparatus*; Report Number: CERN-SPSC-2016-031; SPSC-P-325-ADD-1; CERN: Geneva, Switzerland, 2016.
4. Surko, C.M.; Greaves, R.G.; Charlton, M. Stored positrons for antihydrogen production. *Hyperfine Interact.* **1997**, *109*, 181–188. [CrossRef]
5. Baker, C.J.; Bertsche, W.; Capra, A.; Cesar, C.L.; Charlton, M.; Christensen, A.J.; Collister, R.; Cridland Mathad, A.; Eriksson, S.; Evans, A.; et al. Design and performance of a novel low energy multispecies beamline for an antihydrogen experiment. *Phys. Rev. Accel. Beams* **2023**, *26*, 040101. [CrossRef]
6. Ahmadi, M.; Baquero-Ruiz, M.; Bertsche, W.; Butler, E.; Capra, A.; Carruth, C.; Cesar, C.L.; Charlton, M.; Charman, A.E.; Eriksson, S.; et al. An improved limit on the charge of antihydrogen from stochastic acceleration. *Nature* **2016**, *529*, 373–376. [CrossRef] [PubMed]
7. Amole, C.; Andresen, G.B.; Ashkezari, M.D.; Baquero-Ruiz, M.; Bertsche, W.; Butler, E.; Cesar, C.L.; Chapman, S.; Charlton, M.; Deller, A.; et al. Discriminating between antihydrogen and mirror-trapped antiprotons in a minimum-B trap. Antihydrogen and mirror-trapped antiproton discrimination: Discriminating between antihydrogen and mirror-trapped antiprotons in a minimum-B trap. *New J. Phys.* **2012**, *14*, 105010. [CrossRef]
8. Hodgkinson, D. On the Dynamics of Adiabatically Cooled Antihydrogen in an Octupole-Based Ioffe-Pritchard Magnetic Trap. Ph.D. Thesis, The University of Manchester, Wetzlar, Germany, 2022.
9. Zhong, M.; Fajans, J.; Zukor, A. Axial to transverse energy mixing dynamics in octupole-based magnetostatic antihydrogen traps. *New J. Phys.* **2018**, *20*, 053003. [CrossRef]
10. Hoecker, A.; Speckmayer, P.; Stelzer, J.; Therhaag, J.; von Toerne, E.; Voss, H.; Backes, M.; Carli, T.; Cohen, O.; Christov, A.; et al. TMVA—Toolkit for Multivariate Data Analysis. *arXiv* **2007**, arXiv:0703039.
11. Stan Development Team. Stan Modeling Language Users Guide and Reference Manual, 2.32. Available online: https://mc-stan.org (accessed on 12 July 2023).
12. Hoffman, M.D.; Gelman, A. The No-U-Turn Sampler: Adaptively Setting Path Lengths in Hamiltonian Monte Carlo. *J. Mach. Learn. Res.* **2014**, *15*, 1593–1623.
13. Urioni, M. (University of Brescia, Brescia, Italy); Stracka, S. (INFN Pisa, Pisa, Italy); Bonomi, G. (University of Brescia, Brescia, Italy). Unpublished work, 2023.